REMARKS

The amendment filed August 22, 2005 was not entered, so the present changes are based on the claims as they appear in the Amendment filed November 26, 2004. Claims 51 - 72 remain active in the case. Claim 73 has been cancelled as redundant in view of amended claim 51.

Support for classifying a test substance in one or more functional categories based on reference to a data library formed from known compounds is found on page 30, lines 11 – 12; page 31, lines 7 – 15; page 32, Table 1 and page 33, lines 1 - 17.

Serum-free culture medium is supported on page 26, lines 4 – 6 ("The neurons are grown...in serum-free media. The cells are cultured in defined media...").

An intervening layer acting as a high-impedance seal is supported in the specification at page 11, lines 6 – 12.

Measurement of changes in one or more characteristics selected from after potential, time to cessation of activity, frequency, amplitude, shape, spike rate, or time constant are described on page 40, lines 14 – 31 and this subject matter was also in claim 53.

Deconvoluting changes to identify one or more ion channels affected by the test substance is supported on page 7, lines 13 – 28 and page 10, lines 4 – 16. Please note we specifically define deconvolution as not including spectral analysis on page 13, lines 1 – 5. Therefore, the term "deconvolution" does not read on Fourier Transform analysis.

Our initial description of "functional categories" came from the literature (see ref Riley et at in the application as well as page 6 lines 17-18) and it is a method of classifying related genes and their gene products and thus the pathways they enable. We have shown differences in Action Potential peak shape with the data included in the application, see Figure 5.

We have since demonstrated the application in our paper "Toxin Detection based on Action Potential Peak Shape Analysis using a Realistic Mathematical Model of Differentiated NG106-15 Cells" that has been accepted and is in press in the journal Biosensors and Bioelectronics (Mohan, et al., submitted herewith).

Table 1 on page 32 of the application also further illustrates our ability to group the effects of different compounds into different "functional categories".

As discussed on page 40 lines 21-32 and page 41 lines 1-4 of the application, deconvolution of an action potential implies that some prior knowledge of the factors contributing to the shapes are known. It is well known that an action potential requires the contributions of ion fluxes through at least three distinct ion channels. Varying the contributions of these ion fluxes from these channels has been shown to very the shape of the action potential, and this is illustrated in Figures 5 and 6A. of the application. Thus, to deconvolute an action potential into its components and relate them to pathways or functional categories inside a cell requires some prior knowledge of the biology of the system (i.e., a data base of biological test data on the subject cell culture) in order to perform the deconvolution step and identify cell pathways. The Mohan, et al. paper illustrates some of our efforts in this area and an implementation of the algorithm shown in Figure 10 of the patent application. This algorithm has been used to deconvolute one of the examples given in Figure 5 of the application and is shown in Figure A, below.

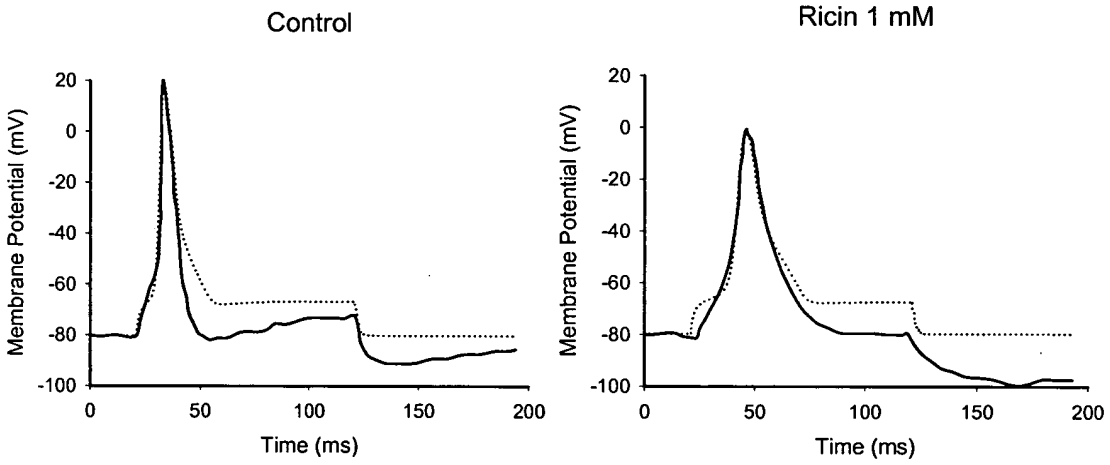

Figure A. Result of parameter fitting to action potential shapes before (left panel) and after (right panel) the application of 1 mM Ricin. Action potentials were recorded from differentiated NG108-15 cells using whole-cell patch clamp method. Action potentials was fitted (dotted lines) with a computer model of NG108-15 cells established based on the measurement of ion channel parameters.

Control	Activation					Inactivation				
	g	V_{Rev}	z	$V_{1/2}$	(	A	z	$V_{1/2}$	(	A
Na	140.00	100.00	6.00	-59.93	-0.45	1.80	-7.48	-70.36	0.42	8.00
K	26.00	-80.00	8.00	-10.00	-0.60	10.00				
Ca	11.00	32.00	4.10	-11.00	-0.67	0.47				
Ricin										
Na	**75.00**	100.00	6.00	-59.93	-0.42	**3.00**	-7.48	-70.36	0.42	**12.00**
K	26.00	-80.00	8.00	-10.00	-0.60	**15.00**				
Ca	11.00	32.00	4.10	-11.00	-0.67	**0.80**				

Table 1. Effect of 1 mM Ricin on the action potential parameters. Action potential parameters were obtained by fitting the parameters of our NG108-15 cell model to the experimental data. 1 mM Ricin caused a significant slow-down of the sodium channel kinetics (parameter A) and a decrease of sodium conductances in the membrane (parameter g). The effect of Ricin on the other ion channels were not so profound, partly because potassium and calcium channels are activated at higher membrane potentials, so their contribution to the Ricin-modified action potential is less (the amplitude of the action potential is smaller, barely reaching 0 mV).

This type of analysis is very different than a spectral analysis "i.e. a Fortier Transform" which arbitrarily assigns combinations of sign waves of different frequencies and amplitudes, to represent the area under a curve. The assignment of the different sign waves is arbitrary and, although it gives a unique signature to a signal, there is no way to relate it to biological information, except through an empirical approach to the testing of drugs or other compounds as well as toxic chemicals.

Claims 51 – 67 and 70 - 73 are rejected under 35 USC 103(a) over Borkholder et al. in view of Georger, Jr. et al.

Borkholder et al. does not specifically disclose an intervening layer, as claimed. Furthermore, it does not disclose or suggest serum-free media. Finally, it does not inherently disclose a deconvolution analysis based on a data library, as claimed. Instead it mentions that a "pattern of spectral changes provides a unique *signature* for the compound. Matching the spectral change pattern of a test compound with the spectral change pattern for reference compounds provides a useful method for characterization of channel modulating agents." (Col. 4, lines 15 – 20, emphasis added). This passage describes using the observed changes as a fingerprinting method to associate certain channel-modulating compounds with the observed changes, but that is not the same kind of process as deconvoluting a signal to identify the

contributions of different ion channels to the signal and then to assigne the test compound to one or more a functional categories.

Georger Jr. et al. teaches a method of making biosensors using photolithography placement techniques. It never explicitly states that a high-impedance seal is created or that it would enable deconvolution. For instance, col. 7, lines 58 – 63 does not relate to deconvolution, but at most implies a high-impedance seal. Col. 10, lines 58 – 62 describes manual placement, whereas we deposit the cells by cell culture. At col. 13, lines 19 – 24, the cell culture patterning method is to use fewer steps. The discussions at col 16, line 45 and at col. 10, lines 50 – 65 relate to positioning.

Finally, Georger Jr. et al. uses serum (col. 17, lines 60 – 65) and states at col. 18, lines 9 – 10 that "adhesion is unaffected by serum." Especially where high-throughput screening is involved, the absence of serum is vital.

Claims 51 – 73 are rejected under 35 USC 12, first paragraph, for written description problems. Support for the high-impedance intervening layer allowing deconvolution as claimed is found on page 11, lines 6 – 12.

Claim 51 is rejected under 35 USC 12, first paragraph, on enablement grounds. A positive deconvolution step is now recited.

Claims 51 – 73 are rejected under 35 USC 12, second paragraph, as being indefinite for failure to positively recite a deconvolution step. This has been address by amendment.

Claim 57 has been clarified with respect to the position of the insulator "surrounding" the electrode.

The dependency of claim 61 has been corrected.

Claim 67 does add a limitation over claim 66 because "known function" and "unknown function" are not the only two possibilities for DNA; some DNA has no function at all.

Applicants submit the case is now in condition for allowance.

Respectfully submitted,

Gilberto M. Villacorta, PH.D.
Registration No. 34,038
Robert W. Hahl, PH.D.
Registration No. 33,893

Enclosures: RCE Transmittal Form and Check #1204 for $905.00
Cited Reference "Mohan et al."

Date: **January 23, 2006**

Patent Administrator
KATTEN MUCHIN ROSENMAN LLP
525 West Monroe Street
Chicago, Illinois 60661-3963
Fax: (312) 906-1021
(202) 625-3500

Available online at www.sciencedirect.com
SCIENCE DIRECT
ELSEVIER
Biosensors and Bioelectronics xxx (2005) xxx–xxx
BIOSENSORS & BIOELECTRONICS
www.elsevier.com/locate/bios

Toxin detection based on action potential shape analysis using a realistic mathematical model of differentiated NG108-15 cells

Dinesh K. Mohan [b], Peter Molnar [a,b], James J. Hickman [a,b,*]

[a] *Nanoscience Technology Center, University of Central Florida, 12424 Research Parkway, Suite 400, Orlando, FL 32826, USA*
[b] *Department of Electrical Engineering, Clemson University, Clemson, SC 29634, USA*

Received 22 April 2005; received in revised form 21 July 2005; accepted 16 September 2005

Abstract

The NG108-15 neuroblastoma/glioma hybrid cell line has been frequently used for toxin detection, pharmaceutical screening and as a whole-cell biosensor. However, detailed analysis of its action potentials during toxin or drug administration has not been accomplished previously using patch clamp electrophysiology. In order to explore the possibility of identifying toxins based on their effect on the shape of intracellularly or extracellularly detected action potentials, we created a computer model of the action potential generation of this cell type. To generate the experimental data to validate the model, voltage dependent sodium, potassium and high-threshold calcium currents, as well as action potentials, were recorded from NG108-15 cells with conventional whole-cell patch-clamp methods. Based on the classic Hodgkin–Huxley formalism and the linear thermodynamic description of the rate constants, ion-channel parameters were estimated using an automatic fitting method. Utilizing the established parameters, action potentials were generated in the model and were optimized to represent the actual recorded action potentials to establish baseline conditions. To demonstrate the applicability of the method for toxin detection and discrimination, the effect of tetrodotoxin (a sodium channel blocker) and tefluthrin (a pyrethroid that is a sodium channel opener) were studied. The two toxins affected the shape of the action potentials differently and their respective effects were identified based on the changes in the fitted parameters. Our results represent one of the first steps to establish a complex model of NG108-15 cells for quantitative toxin detection based on action potential shape analysis of the experimental results.

Keywords: Action potential shape analysis; Toxin detection; NG108-15; Computer simulation; Linear thermodynamic model; Hodgkin–Huxley model

1. Introduction

In the areas of environmental protection, toxicology and drug development there are increasing demands for high-throughput functional screening methods (Rogers, 1995; Paddle, 1996; Ohlstein et al., 2000; Heck et al., 2001; Croston, 2002; Tzoris et al., 2002). For monitoring of the environment, whole-cell biosensors could be more effective than physico-chemical methods to assess the global toxicity of the wide variety of chemicals that are possible pollutants (Evans et al., 1986; Rogers, 1995; Bousse, 1996; Paddle, 1996; Naessens and Tran-Minh, 1998a,b). Whole-cell biosensors are also able to give functional information about the effect of chemicals, have the ability to detect unknown compounds and continuous monitoring of external conditions is possible as they can be made small enough to allow field applications (Bousse, 1996). Another benefit of whole cells in environmental applications is that they allow the measurement of the total bioavailability of a given pollutant rather than its free form (Bousse, 1996; Naessens and Tran-Minh, 1998a,b; Philp et al., 2003). Similarly, in safety pharmacology, the side effect spectrum of a given compound is not known, thus, the application of complex functional tests at the whole-organism-level are necessary (Jorkasky, 1998; Kinter and Valentin, 2002) and could be addressed with this technique. Moreover, the availability of genomic information significantly increased the number of potential targets available for drug discovery and new methods are necessary for high-throughput functional screening for target validation (Ohlstein et al., 2000; Croston, 2002).

Recently, the application of whole-cell biosensors for toxin detection and drug screening has become more readily accepted (Bousse, 1996; Bentleya et al., 2001; Baeumner, 2003) as it has many benefits compared to traditional methods of evaluation. Several techniques have been developed to quantify the physiological changes induced by chemicals in whole-cell

* Corresponding author. Tel.: +1 864 710 8472; fax: +1 407 882 1156.
E-mail address: jhickman@mail.ucf.edu (J.J. Hickman).

0956-5663/$ – see front matter © 2005 Elsevier B.V. All rights reserved.
doi:10.1016/j.bios.2005.09.008

biosensors (Bousse, 1996; Bentleya et al., 2001). One of these techniques, which is frequently used for monitoring the physiological state/activity of excitable cells, is multi-electrode extracellular recording of membrane potential (Bousse, 1996; Gross et al., 1997; Denyer et al., 1998; Jung et al., 1998; Offenhausser and Knoll, 2001; Krause et al., 2000; Stett et al., 2003). The high-throughput or long-term application of extracellular recording is much preferred over intracellular action potential recording for many applications because the use of an intra-cellular or patch clamp electrode limits the life of the cell to a few hours as does the use of voltage sensitive dyes (all dyes reported to date, to a greater or lesser extent, are toxic to cells) (Mason, 1993; Chiappalone et al., 2003).

Action potential generation and the shape of the action potential depends on the status of several ion channels located in a cell's membrane, which are regulated by receptors and intracellular messenger systems (Gross et al., 1995, 1997; Morefield et al., 2000). Changes in the extracellular (receptor activation) or intracellular environment (gene expression), in many cases, can be reflected in an alteration of spontaneous firing properties such as the frequency and firing pattern (Gross et al., 1997; Amigo et al., 2003; Chiappalone et al., 2003; Xia et al., 2003) of excitable cells and also in changes in the shape of their action potentials (Clark et al., 1993; Muraki et al., 1994; Akay et al., 1998; Nygren et al., 1998; Djouhri and Lawson, 1999). There are many examples indicating that the shape of action potential depends on the extracellular and intracellular environment of the cells. Sodium (Spencer et al., 2001), potassium (Clark et al., 1993; Martin-Caraballo and Greer, 2000) and calcium channel modulators (Ahmed et al., 1993; van Soest and Kits, 1998), as well as several toxins and various pathological conditions (Muraki et al., 1994; Shaw and Rudy, 1997; Akay et al., 1998; Djouhri and Lawson, 1999) have already been shown to affect the shape of action potentials. However, action potential shape analysis for high-throughput screening applications, such as toxin detection or drug screening, has not yet been developed. Two primary reasons this type of analysis has been lacking to date is that it is difficult to obtain high fidelity recordings from chip-based extracellular electrodes and from the lack of models to adequately analyze the signals.

Several mathematical models have been developed to describe the electrical properties and the process of action potential generation in excitable cells (Agin, 1972; Cohen, 1976; Otten and Scheepstra, 1995; Dokos and Lovell, 1996; Weiss, 1996; Shevtsova et al., 2003). The most widely used is the Hodgkin–Huxley formalism where ion channel activation and inactivation is described using voltage dependent activation and inactivation gates (Weiss, 1996). In the original model the voltage and time dependence of the gates was given utilizing rate constants, which were taken as an empirical function of the membrane potential (Hodgkin and Huxley, 1952). However, in lieu of using empirical functions, it is also possible to deduce the functional form of the voltage dependence of the rate constants from thermodynamics (Weiss, 1996; Destexhe and Huguenard, 2000). The applications of these models to extracellular recordings from a suitable excitable cell population, in combination with the proper models, would be a logical next step in adapting this technology to high throughput toxin detection and drug discovery.

The NG108-15 hybrid cell line, which was created by merging mouse neuroblastoma and rat glioma cells, has been widely used in in vitro experiments as a substitute for primary-cultured neurons (Hu et al., 1997; Doebler, 2000; Tojima et al., 2000). The neuronal functions and features of differentiated NG108-15 cells have been well characterized, e.g. the presence of a wide range of voltage dependent and transmitter activated membrane currents have been detected as well as second messengers and enzymes normally found in primary neurons (Schmitt and Meves, 1995; Lukyanetz, 1998; Ma et al., 1998; Tojima et al., 2000). NG108-15 cells are widely used in pharmacology (Hu et al., 1997) and also as a whole-cell biosensor for toxin detection (Ma et al., 1998). One of the distinctive features of the NG108-15 cell line, which makes it ideal for whole-cell biosensor applications, is that the cells do not form synaptic connections, thus network activity does not influence single cell data (Ma et al., 1999).

In this study we created a computer model of the action potential generation of an NG108-15 cell based on voltage-clamp and current clamp electrophysiological recordings. Using this model we developed and demonstrated the applicability of action potential shape analysis as a method for toxin detection and monitoring the physiological state of excitable cells.

2. Methods

2.1. Surface chemistry

NG108-15 cells were plated on N-1[3-(trimethoxysilyl) propyl]diethylenetriamine (DETA) coated glass coverslips (22 mm × 22 mm, Thomas Scientific). The DETA coated coverslips were prepared according to published protocols (Schaffner et al., 1995). In brief, glass coverslips were cleaned using HCl/methanol (1:1) followed by a concentrated H_2SO_4 soak for 30 min followed by a water rinse. The coverslips were then boiled in deionized water followed by a rinse with acetone and then oven dried. The DETA films were formed by the reaction of the cleaned surfaces with a 0.1% (v/v) mixture of the organosilane in toluene. The DETA cover glasses were heated to just below the boiling point of toluene, rinsed with toluene; reheated to just below the boiling temperature again and then oven dried.

2.2. Culture of NG108-15 cells

The NG108-15 cell line (passage number 16) was obtained from Dr. M.W. Nirenberg (NIH). The NG108-15 cells were cultured according to published protocols (Higashida et al., 1986; Ma et al., 1998). Briefly, the cell stock was grown in T-25 and T-75 flasks in 90% Dulbecco's modified Eagle's medium (DMEM, GIBCO) supplemented with 10% fetal bovine serum and HAT supplement (GIBCO, 100×) at 37 °C with 10% CO_2. Differentiation was induced by plating the cells in a serum-free defined medium (DMEM + N_2 supplement, GIBCO) in 35 mm culture dishes at a density of 40,000 cells/dish.

2.3. Electrophysiological recordings

Whole-cell patch clamp recordings were performed in a recording chamber on the stage of a Zeiss Axioscope 2 FS Plus upright microscope. The chamber was continuously perfused (2 ml/min) with the extracellular solution. The composition of the extracellular solution for the recording of action potentials was (in mM): NaCl 140, KCl 3.5, $MgCl_2$ 2, $CaCl_2$ 2, glucose 10, HEPES 10. For the recording of potassium currents 1 μM tetrodotoxin (TTX) was added to the extracellular solution. To minimize space-clamp errors, sodium currents were recorded in a 'decreased sodium' extracellular solution containing (in mM): NaCl 50, TEA-Cl 100, CsCl 5, $CaCl_2$ 1, $CoCl_2$ 1, $MgCl_2$ 1, glucose 10, HEPES 10. For the recording of calcium currents, sodium and potassium channels were blocked with Cs, TEA and TTX. The extracellular solution composition for the measurement of calcium currents was (in mM): NaCl 100, TEA-Cl 30, $CaCl_2$ 10, $MgCl_2$ 2, glucose 10, HEPES 10, TTX 0.001. The pH was adjusted to 7.3 and the osmolarity was 320 mOsm. The intracellular solutions composition for recording the action potentials and for potassium channel measurements was (in mM): kgluconate 130, $MgCl_2$ 2, EGTA 1, HEPES 15, ATP 5, for sodium channels was CsF 130, NaCl 10, TEA-Cl 10, $MgCl_2$ 2, EGTA 1, HEPES 10, ATP 5 and for calcium channels was: CsCl 120, TEA-Cl 20, $MgCl_2$ 2, EGTA 1, HEPES 10, ATP 5 (pH 7.2; osmolarity = 280 mOsm). For selecting L-type calcium channels, 1 μM ωCT × GVIA was used.

Patch pipettes (4–6 MΩ resistance) were prepared from borosilicate glass (BF150-86-10; Sutter, Novato, CA) with a Sutter P97 pipette puller. Voltage clamp and current clamp experiments were performed with a Multiclamp 700A (Axon, Union City, CA) amplifier. Signals were filtered at 2 kHz and digitized at 20 kHz with an Axon Digidata 1322A interface. Data recording and analysis was performed using pClamp 8 (Axon) software. Sodium and potassium currents were measured in voltage clamp mode using 10 mV voltage steps from a −85 mV holding potential. To record high-threshold calcium currents, a −40 mV holding was used. Whole cell capacitance and series resistance was compensated and a p/6 protocol was used. The access resistance was less than 22 MΩ. Action potentials were measured in current-clamp mode using 1 s depolarizing current injections. Data was saved in text-format and imported into MATLAB for further analysis.

2.4. Simulation of ionic conductances and action potential generation in NG108-15 cells

The classic Hodgkin–Huxley model (Hodgkin and Huxley, 1952) was used for the description of the ion channel currents, but instead of the original empirical description of the rate constant, the thermodynamic approach (Weiss et al., 1995; Destexhe and Huguenard, 2000) was applied. Briefly, the total ionic membrane current was described as:

$$I_{\text{ionic}} = I_{\text{Na}} + I_{\text{K}} + I_{\text{Ca}} + I_{\text{l}} = \bar{g}_{\text{Na}} m^3 h (V - V_{\text{Na}}) + \bar{g}_{\text{K}} n^4 (V - V_{\text{K}}) + \bar{g}_{\text{CaL}} e^3 (V - V_{\text{CaL}}) + \bar{g}_{\text{l}} (V - V_{\text{l}})$$

dynamic changes in the membrane-potential were calculated according to:

$$\frac{dV}{dt} = \frac{I_{\text{external}} - I_{\text{ionic}}}{C_{\text{M}}}$$

The dynamics of the state variables was given as $dm/dt = (m_\infty - m)/\tau_{\text{m}}$. Where $\bar{g}_{\text{Na}}$, $\bar{g}_{\text{K}}$, $\bar{g}_{\text{CaL}}$, V_{Na}, V_{K}, V_{CaL} are constants (maximum conductances of the channels and reversal potentials, respectively); m, n, h, e are the state variables, m_∞, n_∞, h_∞, e_∞ are the steady-state values of the state variables and the τ-s are their voltage-dependent time-constants. The voltage-dependence of the steady-state state parameters and the time constants were given using the general thermodynamic formalism (using the state-variable m as an example):

$$m_\infty = \frac{1}{1 + \exp^{-zF/\text{RT}(V_{\text{m}} - V_{1/2})}}$$

and

$$\tau_m = \frac{A}{\exp^{(zF/\text{RT})\xi(V_{\text{m}} - V_{1/2})} \cos h(zF/2\text{RT}(V_{\text{m}} - V_{1/2}))}$$

where z, $V_{1/2}$, A and ξ are fitting parameters and V_{m} represents the membrane potential.

As it can be seen from these equations $V_{1/2}$ corresponds to the half activation/inactivation potential of the channel and A is linearly related to the activation or inactivation time-constant. The meanings of z and ξ are not as obvious: z is related to the number of moving charges during the opening or closing of the channel; whereas ξ describes the asymmetric position of the moving charge in the cell membrane. Sodium, potassium and calcium channel mediated currents, which were recorded in voltage-clamp mode at different membrane potentials (10 mV increments, −40 mV, +30 mV range), were fitted in one step using the above described model, with the corresponding ion channels included, using the built-in routines (fminunc) of MATLAB through a custom-made graphical interface. Parameters obtained from different cells were averaged ($n = 4$–6) and considered as initial values for the action potential modeling. Simulated action potentials were fitted to the experimental data using built-in functions in MATLAB (fminunc). Fminunc is used to find a minimum of a scalar function (the error function, see Section 3) of several variables, starting at an initial estimate. This method is generally referred to as unconstrained nonlinear optimization. Because it is finding only local minimums, it is very important to start the optimization as close to the final result as it is possible. In our case, the averaged ion channel parameters obtained from voltage clamp experiments served the initial values for the parameter estimations.

3. Results

The NG108-15 cells completed their differentiation process and a neuronal phenotype was obtained by day 10 in vitro (DIV) in the defined, serum-free medium (Fig. 1A). Electrophysiological experiments were performed on the differentiated cells between day 10 and 14 in vitro. All of the cells investigated showed pronounced sodium, potassium and calcium currents in

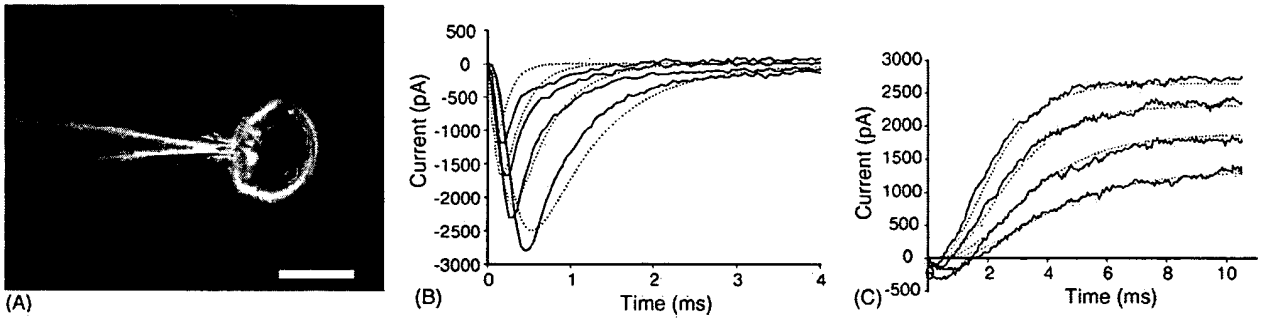

Fig. 1. Estimation of ion channel parameters from the voltage-clamp experiments. (A) Phase-contrast picture of an NG108-15 cell with a patch-clamp electrode attached to the cell (40× objective, scale bar = 25 μm). (B) Sodium currents recorded at different membrane potentials of −10, 0, 10, 20 mV in voltage-clamp mode (solid line) and the results of the parameter fitting using the Hodgkin–Huxley model and the linear thermodynamic formalism (dotted line). (C) Potassium currents recorded at membrane potentials of 0, 10, 20 and 30 mV (solid line) and the fitted curves using the model (dotted line).

the voltage-clamp experiments. Most of the cells fired one single action potential upon depolarization in current-clamp mode, whereas about 10% of the cells were able to fire multiple action potentials. Only a very small minority of the cells (about 5%) were spontaneously active.

3.1. Extracting ion-channel parameters from the voltage-clamp experiments using the linear thermodynamic description

Signals from sodium, potassium and high-threshold (L-type) calcium channels were recorded in voltage-clamp mode using the Axon's pClamp 8 program with standard protocols (Fig. 1B and C). The data were saved in ASCII format and imported into the MATLAB program. A graphical interface was created to fit the mathematical model to the experimental data and to visualize the results. To quantify the difference between the fitted curves and the recorded data the following error-functions were implemented:

1. Maximum error: $E_{\mathrm{Max}} = \mathrm{Max}(\mathrm{Abs}(R(t_n) - S(t_n)))$ where $R(t_n)$ is the recorded value and $S(t_n)$ is the simulated data at time t_n.
2. Least square: $E_{\mathrm{Lsquare}} = \sum_n (R(t_n) - S(t_n))^2$.
3. Weighted least square: $E_{\mathrm{WLsquare}} = E_{\mathrm{Lsquare}}$ if $t_n < 30$ ms and $E_{\mathrm{WLsquare}} = 5 \times E_{\mathrm{Lsquare}}$ if $t_n \geq 30$ ms.

After several trials it was concluded that simulations using the weighted least square error function gave the most satisfactory results because the other error functions occasionally obtained a non-inactivating sodium-current component in the simulated data. Curves were fitted after an initial 0.1 ms delay to eliminate the effect of experimental artifacts. In some simulations the reversal potential for the ionic conductances was kept constant.

In general, an excellent fit to the potassium channel data (Fig. 1B and C) and an acceptable fit to the sodium and calcium channel data were achieved. The automatic fitting algorithm converged in less than 2 min running on a Pentium III 1 GHz personal computer. After averaging the results of 3–10 experiments the initial parameter values for modeling the action potentials were obtained (Table 1).

3.2. Action potential shape analysis

Action potentials were evoked with short (2 ms) current injections in current clamp mode either at resting membrane potential or at a −85 mV holding potential. The following parameters were obtained from the patch-clamp recordings and used in the modeling: membrane resistance, resting membrane potential, membrane capacitance and injected current. The maximum conductance of the leakage current (g_l) was calculated from the ionic conductances and from the resting membrane potential. We used the earlier established, averaged ion-channel parameters as the initial parameters for the action potential fitting. Using voltage dependent sodium, potassium and L-type calcium onductances, an excellent fit to the rising and to the initial falling phase of the action potentials in the NG108-15 cells was obtained (Fig. 2).

We also obtained an excellent fit to the experimental data in the case of the toxin-modified action potentials by modifying only the corresponding sodium-channel parameters (Fig. 2, Table 2).

4. Discussion

We have developed a mathematical model of the action potential generation in NG108-15 cells and extracted the parameters for this model from whole-cell patch clamp experiments. Utilizing only voltage-sensitive sodium, potassium and L-type calcium channels we were able to obtain an excellent fit to the rising as well as to the initial falling phase of the action potential. The weak fit to the later falling phase of the action potential could be due to active conductances, which were not taken into account in this model. For example, at lease three other calcium channels and also a calcium activated potassium channel have already been described in NG108-15 cells. In this study, we kept the number of the ion channels modeled to a minimum, due to the high computational requirements of the parameter fitting program.

A linear thermodynamic formalism was used to describe the voltage and time dependence of the ionic conductances, which eliminated the need for 'guessing' the function for the voltage-dependence of the rate constants and the same form (with dif-

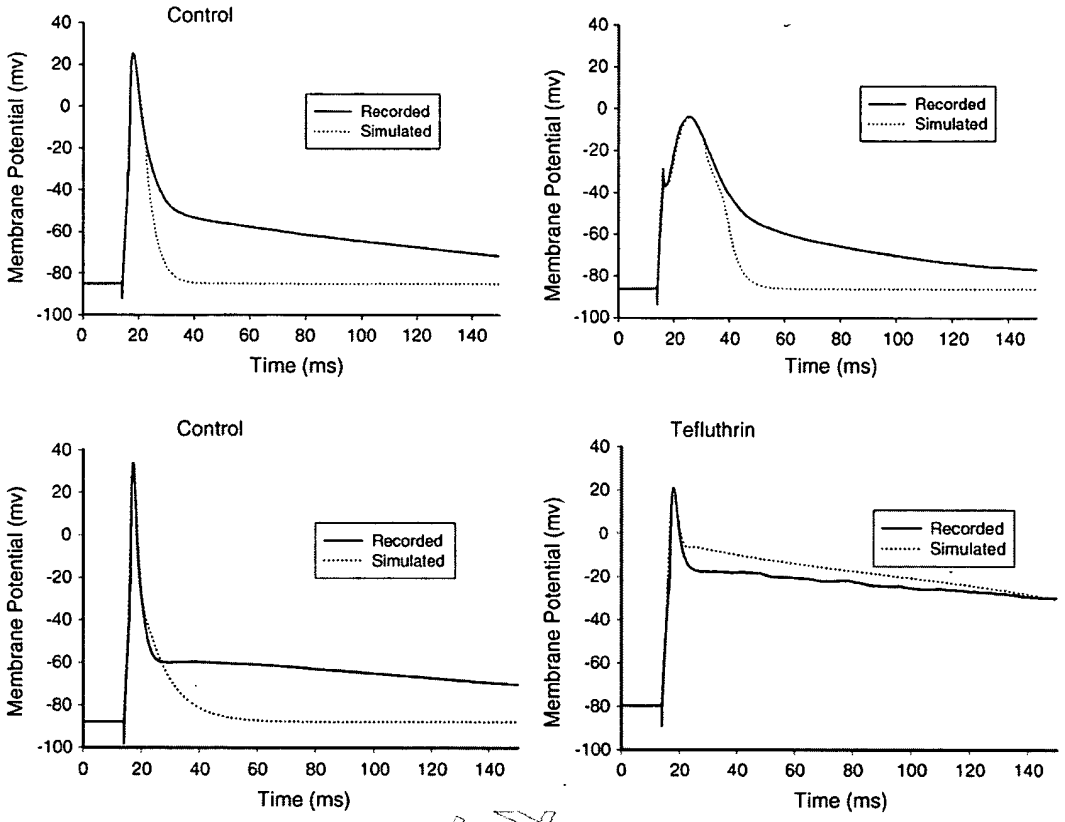

Fig. 2. Effect of toxins on the action potentials of NG108-15 cells. (Upper panel) effect of 0.5 μM tetrodotoxin. (Lower panel) effect of 0.5 μM tefluthrin. (Solid line) data recorded in current clamp experiments. (Dotted line) results of the simulation using the mathematical model of the NG108-15 cells.

ferent parameters) could be used for the characterization of all the ion channels.

One of the limitations of the model is the high number of parameters required to describe the ionic conductances. In this study four parameters were used to characterize each activation/inactivation gate, thus, for the description of the sodium channel, a total of 10 parameters was required. With this high number of parameters a more detailed study is needed to prove the uniqueness and stability of the solutions.

In order to validate the action potential shape analysis for utilization as a toxin detection method, the effect of two toxins, tetrodotoxin, a specific sodium channel blocker, and tefluthrin, a sodium channel opener pyrethroid were analyzed. Changes in the action potential shape, and also in the fitted ion-channel parameters caused by the two toxins, were measured. An excellent fit to the toxin-modified action potential shapes by modifying only the appropriate sodium channel parameters has been achieved. TTX, as expected from a channel blocker, significantly decreased the maximum sodium conductance (g), but did not affect the voltage dependence of the channel ($V_{1/2}$) (Table 2). Unexpectedly, TTX affected the activation kinetics of the sodium channels as well. TTX moderately increased the activation A parameter by causing a slowing down of the activation of the channel. One possible explanation could be the existence of different subpopulations of sodium channels on the NG108-15 cells with different activation and inactivation time constants and different TTX sensitivities.

The major effect of tefluthrin (a channel opener) was to slow down (practically remove) the inactivation of the sodium channels (A). Tefluthrin also affected the maximum sodium channel conductance (g) and the voltage dependence of the activation and inactivation of the channel ($V_{1/2}$), shifting appropriate current–voltage (I/V) relationships to the left by about 15 mV. A Similar effect on the voltage dependence of the sodium channels was described by Spencer et al. (2001) for fenpropathrin, a tefluthrin-like pyrethroid.

In summary, these experiments indicated that we were able to decipher and quantify the effects of toxins on ion channels without actually measuring ion channel currents in voltage-clamp experiments. Instead, changes in the shape of action potentials measured by patch clamp electrophysiology, combined with a validated computer simulation of the cell, were utilized.

This method could be useful for toxin detection and for classification of unknown toxins in environmental protection scenarios or in the detection of biological and chemical warfare agents. It could also be extended to functional screening in drug development. With the refinement of the model of the cell not only those toxins could be identified, which are directly acting on ion channels, but also changes in second messenger levels or gene expression could also be detected and classified. Moreover,

Table 1
Average ion channel parameters characteristic of NG108-15 cells obtained by parameter fitting to voltage-clamp data ($n=3$–10)

Channel	g	S.E.M.	V_{Rev}	S.E.M.	Activation								Inactivation							
					z	S.E.M.	$V_{1/2}$	S.E.M.	ξ	S.E.M.	A	S.E.M.	z	S.E.M.	$V_{1/2}$	S.E.M.	ξ	S.E.M.	A	S.E.M.
Sodium	343.59	183.23	72.35	6.31	5.98	0.30	−46.93	2.46	−0.38	0.01	0.58	0.12	−7.48	1.13	−64.36	4.73	0.41	0.01	1.31	0.17
Potassium	25.09	4.81	−80.00	0.00	2.78	0.46	−22.52	2.64	−0.26	0.02	2.12	0.16								
Calcium	7.45	1.88	32.00	0.00	3.15	0.96	−4.67	6.25	−0.30	0.37	0.84	0.37								
Leakage	5.22	0.89	−49.40	0.76																

S.E.M.: standard error of mean, V_{Rev}: reversal potential.

Table 2
Effect of TTX and tefluthrin on the action potential parameters

Na	g	V_{Rev}	Activation				Inactivation			
			z	$V_{1/2}$	ξ	A	z	$V_{1/2}$	ξ	A
Control	317 ± 84	60	6 ± 0.04	−6.9 ± 0.3	−0.38 ± 0.03	0.59 ± 0.08	−7.5 ± 0.04	−64 ± 0.4	0.43 ± 0.03	1.5 ± 0.7
TTX	31 ± 18	60	6 ± 0.01	−6.9 ± 0.3	−0.40 ± 0.03	0.83 ± 0.17	−7.5 ± 0.1	−64 ± 0.4	0.42 ± 0.02	3.0 ± 0.9
% Change	**−89 ± 6**	0	−0.6 ± 0.6	0 ± 0.004	5.9 ± 5.2	**41 ± 25.5**	0 ± 0.002	0 ± 0.001	−0.68 ± 0.7	331 ± 301
Control	227 ± 106	60	5.6 ± 0.4	−46.7 ± 0.2	−0.38 ± 0	0.7 ± 0.12	−7.4 ± 0.1	−60 ± 2.6	0.48 ± 0.01	1.3 ± 0.22
Tefluthrin	44.6 ± 11	60	5.6 ± 0.4	−54 ± 2.3	−0.36 ± 0.02	1.5 ± 0.6	−7.8 ± 0.3	−69 ± 2.1	0.47 ± 0.04	39 ± 18
% Change	**−71 ± 9**	0	1 ± 1	**17 ± 5**	−4 ± 4.2	86 ± 66	6 ± 5.71	**15 ± 2.2**	−2 ± 7.9	**4410 ± 2974**

Only sodium channel parameters are shown, the other ion-channel parameters did not change. Data shown as mean ± S.E.M., values in bold show statistically significant ($p>0.05$) change.

recent advancements in the study of the cell electrode interface and microelectrode-fabrication technology indicate that high-fidelity extracellular recording of action potential shapes might be possible, which opens a new horizon for the high-throughput application of our method using extracellular recordings.

5. Conclusions

We have demonstrated that toxin effects on ionic membrane currents can be quantified based on the measurement of changes in action potential shape and a realistic mathematical model of action potential generation in NG108-15 cells. Further studies are underway to improve the mathematical model, explore the applicability of the method for detection and identification of a wider variety of toxins and to extend the technique to enable obtaining high-fidelity action potential data with non-invasive, high-throughput extracellular electrodes, in order to make high-throughput functional toxin detection and drug screening possible.

Acknowledgements

The Hunter endowment at Clemson University and DOE grant number DE-FG02-00ER45856 for funding the study; Dr. M.W. Nirenberg (NIH) for kindly supplying the NG108-15 cell line. Initial experiments were done at Clemson University as indicated by the dual affiliations of Drs. Molnar and Hickman.

References

Agin, D., 1972. Excitability phenomena in membranes. In: Rosen, R. (Ed.), Foundations of Mathematical Biology. Academic Press, New York, pp. 253–277.

Ahmed, I.A., Hopkins, P.M., et al., 1993. Caffeine and ryanodine differentially modify a calcium-dependent component of soma action-potentials in identified molluscan (*Lymnaea stagnalis*) neurons in-situ. Comp. Biochem. Physiol. C: Pharmacol. Toxicol. Endocrinol. 105 (3), 363–372.

Akay, M., Mazza, E., et al., 1998. Non-linear dynamic analysis of hypoxia-induced changes in action potential shape in neurons cultured from the rostral ventrolateral medulla (RVLM). FASEB J. 12 (4), 2881.

Amigo, J.M., Szczepanski, J., et al., 2003. On the number of states of the neuronal sources. Biosystems 68 (1), 57–66.

Baeumner, A.J., 2003. Biosensors for environmental pollutants and food contaminants. Anal. Bioanal. Chem. 377 (3), 434–445.

Bentleya, A., Atkinsona, A., et al., 2001. Whole cell biosensors—electrochemical and optical approaches to ecotoxicity testing. Toxicol. In Vitro 15, 469–475.

Bousse, L., 1996. Whole cell biosensors. Sens. Actuators B: Chem. 34 (1-3), 270–275.

Chiappalone, M., Vato, A., et al., 2003. Networks of neurons coupled to microelectrode arrays: a neuronal sensory system for pharmacological applications. Biosens. Bioelectron. 18, 627–634.

Clark, R.B., Bouchard, R.A., et al., 1993. Heterogeneity of action-potential wave-forms and potassium currents in rat ventricle. Cardiovasc. Res. 27 (10), 1795–1799.

Cohen, H., 1976. Mathematical developments in Hodgkin–Huxley theory and its approximations. In: Levin, S.A. (Ed.), Proceedings of the Ninth Symposium on Mathematical Biology. New York, January 1975. American Mathematical Society, Washington, pp. 89–124.

Croston, G.E., 2002. Functional cell-based uHTS in chemical genomic drug discovery. Trends Biotechnol. 20 (3), 110–115.

Denyer, M.C.T., Riehle, M., et al., 1998. Preliminary study on the suitability of a pharmacological bio-assay based on cardiac myocytes cultured over microfabricated microelectrode arrays. Med. Biol. Eng. Comput. 36 (5), 638–644.

Destexhe, A., Huguenard, J.R., 2000. Nonlinear thermodynamic models of voltage-dependent currents. J. Comput. Neurosci. 9, 259–270.

Djouhri, L., Lawson, S.N., 1999. Changes in somatic action potential shape in guinea-pig nociceptive primary afferent neurones during inflammation in vivo. J. Physiol.: Lond. 520 (2), 565–576.

Doebler, J.A., 2000. Effects of neutral ionophores on membrane electrical characteristics of NG108-15 cells. Toxicol. Lett. 114 (1-3), 27–38.

Dokos, S.C., Lovell, B., 1996. Ion currents underlying sinoatrial node pacemaker activity: a new single cell mathematical model. J. Theor. Biol. 181 (3), 245–272.

Evans, G.P., Briers, M.G., et al., 1986. Can biosensors help to protect drinking-water. Biosensors 2 (5), 287–300.

Gross, G.W., Harsch, A., et al., 1997. Odor, drug and toxin analysis with neuronal networks in vitro: extracellular array recording of network responses. Biosens. Bioelectron. 12 (5), 373–393.

Gross, G.W., Rhoades, B.K., et al., 1995. the use of neuronal networks on multielectrode arrays as biosensors. Biosen. Bioelectron. 10 (6–7), 553–567.

Heck, D.E., Roy, A., et al., 2001. Nucleic acid microarray technology for toxicology: promise and practicalities. Biological Reactive Intermediates Vi 500, 709–714.

Higashida, H., Streaty, R.A., et al., 1986. Bradykinin-activated transmembrane signals are coupled via No or Ni to production of inositol 1,4,5-trisphosphate, a 2nd messenger in Ng108-15 neuroblastoma glioma hybrid-cells. Proc. Natl. Acad. Sci. U.S.A. 83 (4), 942–946.

Hodgkin, L.A., Huxley, F.A., 1952. A quantitative description of membrane current and its application to conduction and excitation in nerve. J. Physiol. 117, 500–544.

Hu, Q., Huang, F., et al., 1997. Inhibition of Toosendanin on the delayed rectifier potassium current in neuroblastoma X glioma NG108-15 cells. Brain Res. 751, 47–53.

Jorkasky, D.K., 1998. What does the clinician want to know from the toxicologist? Toxicol. Lett. 102–103, 539–543.

Jung, D.R., Cuttino, D.S., et al., 1998. Cell-based sensor microelectrode array characterized by imaging x-ray photoelectron spectroscopy, scanning electron microscopy, impedance measurements, and extracellular recordings. J. Vac. Sci. Technol. A: Vac. Surf. Films 16 (3), 1183–1188.

Kinter, L.B., Valentin, J.P., 2002. Safety pharmacology and risk assessment. Fundam. Clin. Pharmacol. 16 (3), 175–182.

Krause, M., Ingebrandt, S., et al., 2000. Extended gate electrode arrays for extracellular signal recordings. Sens. Actuators B 70, 101–107.

Lukyanetz, E.A., 1998. Diversity and properties of calcium channel types in NG108-15 hybrid cells. Neuroscience 87 (1), 265–274.

Ma, W., Grant, G.M., et al., 1999. Kir 4.1 channel expression in neuroblastoma×glioma hybrid NG108-15 cell line. Dev. Brain Res. 114 (1), 127–134.

Ma, W., Pancrazio, J.J., et al., 1998. Neuronal and glial epitopes and transmitter-synthesizing enzymes appear in parallel with membrane excitability during neuroblastoma X glioma hybrid differentiation. Dev. Brain Res. 106, 155–163.

Martin-Caraballo, M., Greer, J.J., 2000. Development of potassium conductances in perinatal rat phrenic motoneurons. J. Neurophysiol. 83 (6), 3497–3508.

Mason, T.W., 1993. Fluorescent and Luminescent Probes for Biological Activity. Academic Press, London.

Morefield, S.I., Keefer, E.W., et al., 2000. Drug evaluations using neuronal networks cultured on microelectrode arrays. Biosens. Bioelectron. 15 (7–8), 383–396.

Muraki, K., Imaizumi, Y., et al., 1994. Effects of noradrenaline on membrane currents and action-potential shape in smooth-muscle cells from guinea-pig ureter. J. Physiol. Lond. 481 (3), 617–627.

Naessens, M., Tran-Minh, A., 1998a. Whole-cell biosensor for determination of volatile organic compounds in the form of aerosols. Anal. Chim. Acta 364 (1–3), 153–158.

Naessens, M., Tran-Minh, C., 1998b. Whole-cell biosensor for direct determination of solvent vapours. Biosens. Bioelectron. 13 (3–4), 341–346.

Nygren, A., Fiset, C., et al., 1998. Mathematical model of an adult human atrial cell—the role of K^+ currents in repolarization. Circ. Res. 82 (1), 63–81.

Offenhausser, A., Knoll, W., 2001. Cell-transistor hybrid systems and their potential applications. Trends Biotechnol. 19 (2), 62–66.

Ohlstein, E.H., Ruffolo, R.R., et al., 2000. Drug discovery in the next millennium. Ann. Rev. Pharmacol. Toxicol. 40, 177–191.

Otten, E.H., Scheepstra, M., 1995. A model study on the influence of a slowly activating potassium conductance on repetitive firing patterns of muscle spindle primary endings. J. Theor. Biol. 173 (1), 67–78.

Paddle, B.M., 1996. Biosensors for chemical and biological agents of defence interest. Biosens. Bioelectron. 11 (11), 1079–1113.

Philp, J.C., Balmand, S., et al., 2003. Whole cell immobilised biosensors for toxicity assessment of a wastewater treatment plant treating phenolics-containing waste. Anal. Chim. Acta 487, 61–74.

Rogers, K.R., 1995. Biosensors for environmental applications. Biosens. Bioelectron. 10 (6–7), 533–541.

Schaffner, E.A., Barker, L.J., et al., 1995. Investigation of the factors necessary for growth of hippocampal neurons in a defined system. J. Neurosci. Methods 62, 111–119.

Schmitt, H., Meves, H., 1995. Model experiments on squid axons and NG108-15 mouse neuroblastoma * rat glioma hybrid cells. J. Physiol. (Paris) 89, 181–193.

Shaw, R.M., Rudy, Y., 1997. Electrophysiologic effects of acute myocardial ischemia: a theoretical study of altered cell excitability and action potential duration. Cardiovasc. Res. 35 (2), 256–272.

Shevtsova, N.A.P., McCrimmon, K., Rybak, D.R., 2003. Computational modeling of bursting pacemaker neurons in the pre-Bötzinger complex. Neurocomputing 52–54, 933–942.

Spencer, C.I., Yuill, K.H., et al., 2001. Actions of pyrethroid insecticides on sodium currents, action potentials, and contractile rhytm in isolated mammalian ventricular myocytes and perfused hearts. J. Pharmacol. Exp. Ther. 298, 1067–1082.

Stett, A., Egert, U., et al., 2003. Biological application of microelectrode arrays in drug discovery and basic research. Anal. Bioanal. Chem. 377 (3), 486–495.

Tojima, T., Yamane, Y., et al., 2000. Acquisition of neuronal proteins during differentiation of NG108-15 cells. Neurosci. Res. 37, 153–161.

Tzoris, A., Fearnside, D., et al., 2002. Direct toxicity assessment of wastewater: Baroxymeter, a portable rapid toxicity device and the industry perspective. Environ. Toxicol. 17 (3), 284–290.

van Soest, P.F., Kits, K.S., 1998. Conopressin affects excitability, firing, and action potential shape through stimulation of transient and persistent inward currents in mulluscan neurons. J. Neurophysiol. 79 (4), 1619–1632.

Weiss, I., Urbaszek, A., et al., 1995. Simulation of the cardiac action-potentials of various cell-types with account being taken of neural influencing factors. Biomed. Tech. 40 (3), 64–69.

Weiss, T.F., 1996. Cellular Biophysics. The MIT Press, Cambridge, MA.

Xia, Y., Gopal, K.V., et al., 2003. Differential acute effects of fluoxetine on frontal and auditory cortex networks in vitro. Brain Res. 973 (2), 151–160.